U.S. DEPARTMENT OF ENERGY

PNNL-29423

Prepared for the U.S. Department of Energy
under Contract DE-AC05-76RL01830

Ultrasonic Modem

Matthew S. Taubman
Anton S. Sinkov
Raymond Dunn

November 2019

Pacific Northwest
NATIONAL LABORATORY

Proudly Operated by Battelle *Since 1965*

DISCLAIMER

PACIFIC NORTHWEST NATIONAL LABORATORY
operated by
BATTELLE
for the
UNITED STATES DEPARTMENT OF ENERGY
under Contract DE-AC05-76RL01830

Printed in the United States of America

Available to DOE and DOE contractors from
the Office of Scientific and Technical Information,
P.O. Box 62, Oak Ridge, TN 37831-0062
www.osti.gov
ph: (865) 576-8401
fox: (865) 576-5728
email: reports@osti.gov

Available to the public from the National Technical Information Service
5301 Shawnee Rd., Alexandria, VA 22312
ph: (800) 553-NTIS (6847)
or (703) 605-6000
email: info@ntis.gov
Online ordering: http://www.ntis.gov

PNNL-29423

Ultrasonic Modem

Matthew S. Taubman* Anton Sinkov Raymond Dunn

November 2019

Prepared under U.S. Department of Energy Contract DE-AC05-76RL01830

Pacific Northwest National Laboratory
Richland, Washington 99352

*Corresponding author: Matthew.Taubman@pnnl.gov

Executive Summary

The Dual-Path Ultrasonic Modem project funded by DOE office of Environmental Management is an exploratory demonstration with the goal of passing both power and data through a metal barrier such as a container wall using ultrasonic techniques. Piezoelectric transducers operating in the kilohertz to low megahertz can transmit ultrasonic energy readily through solids. Capturing such an ultrasonic transmission with a similar transducer and converting it to electrical energy now opens up the possibility of communicating through thick steel walls, interrogating sensor systems placed within closed vessels or pieces of industrial machinery without the need for wires, holes in the wall, or other intrusive means, and also without the need for batteries or other power source within the closed vessel. This report details the demonstrated operation of a dual ultrasonic link that transmits ultrasonic power at approximately 500 kHz through stainless steel of up to 36 inches in thickness, harvests and stores this energy, then uses it to transmit data back through the metal to be received and recorded externally.

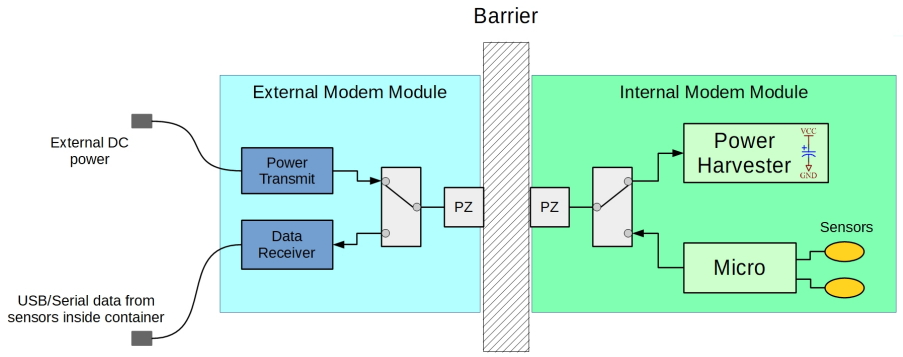

The dual ultrasonic link consists of two parts: an external module and an internal module. The external module contains ultrasonic power transmit and data receive sections. The internal module consists of power harvesting and microcontroller sections. Both modules utilize a piezoelectric (PZ) transducer which is switched to connect to these respective circuits within each module as required by the operating cycle of the system. In this illustration the switches are shown set for power transmission from the external module and power harvesting by the internal module.

A modem operating cycle begins in the external module power-transmit section. This section generates the RF power required to excite the piezo transducer (PZ) to pass ultrasonic energy through the barrier. This power is received by the internal module and stored on a capacitor ready to be used to operate the internal module for data transmission back to the external module. When it has been determined that sufficient

energy has been transferred to the internal module (arbitrarily by the user at this stage of development), the power-transmit circuit is shut down and the PZ switch changed to connect the transducer to the data-receiver circuit, ready to receive data transmissions back through the barrier. Meanwhile, the microcontroller in the internal module detects the cessation of power, switches to directly connect with the internal PZ, commences interrogating the sensors and sends data back through the barrier to the external module for as long as it can on the stored energy it received in the harvesting cycle. When data transmission is complete, the internal system goes into quiescent mode with minimal current draw (< 50 nanoamperes (nA)) ready for subsequent power harvesting.

In our demonstration, the microcontroller transmits data back through the barrier asynchronously, using a specific scheme (discussed in the main body of the report) allowing the use of signals that are not perfectly clean. Each bit-period of the signal is transmitted and interpreted as a 1-bit (an ultrasonic pulse), or 0-bit (the absence of an ultrasonic pulse). Electrical signals derived from the ultrasonic pulses received back through the barrier are only a few millivolts in amplitude. The data receiver amplifies these signals and applies bit-reconstruction techniques so as to produce a reliable bit stream. The resulting data stream is sent serially to a computer connected to the external module. For our demonstration, the data coming from the modem is converted to USB format for ease of interface with common computer systems.

Our system was successfully demonstrated at relatively low input power (a few watts) without the need for large electronic components. The system successfully harvested power and then used the stored energy to measure and transmit simple temperature and voltage data through both 12 and 36 inches of stainless steel. For two watts of power supplied by the power transmit electronics, the power received by the internal electronics was measured to be 4.2 milliwatts (mW) after transmission through a 12-inch stainless steel block, and 1.54 mW for a 36-inch block. The energy accumulated through the 36-inch block in five minutes allowed us to send data back through the block for 4.5 minutes before the storage capacitor in the internal module returned to its initial state of charge before the harvesting cycle.

We feel this proof of principal is a powerful demonstration of the capabilities of this ultrasonic technique. Further work includes testing different barrier materials and shapes, and exploring operating frequency ranges in order to better understand aspects of operating. The above-mentioned measurements were taken without any optimization of voltage to current ratios at the internal measurement point. However, preliminary tests show that by including a peak power tracking technique, improvement by a factor of three in power transfer could be achieved. Parts of the external module presently exist separately, and will be combined onto a single circuit board. It is also proposed that the capabilities of the system be enhanced to automatically identify optimal operational frequencies and amplitudes of ultrasonic power, which depend on the vessel barrier being traversed. Ultimately, we see this system as operating solely from the 48 VDC available over standard Ethernet.

Acronyms and Definitions

°C	degrees Centigrade
Ω	ohm
µH	microhenrys
A	amperes / amps
ASK	amplitude shift keying
BNC	British naval connector
DC	direct current
DOE	Department of Energy
Hz	hertz
kΩ	kilohm
kHz	kilohertz
LC	inductor-capacitor
m/s	meters per second.
MOSFET	metal-oxide-silicon field-effect transistor
mW	milliwatts
nA	nanoamperes
PCB	printed circuit board
pF	picofarads

PZ piezoelectric

RF radio frequency / radio-frequency

TX transfer

UART universal asynchronous receiver/transmitter

VDC volts direct current

Vpp Volts peak-to-peak

W Watts

Contents

List of Figures

1 Introduction

The need exists for the capability of transferring data from sensors through the walls of sealed vessels when electrical penetrations are not permitted or desired. A concurrent requirement is to power the internal sensor circuitry by some means other than a battery. There are multiple reasons for this, including the limited lifetime of batteries, the potentially adverse effects of internal vessel conditions on batteries, as well as the potentially undesirable effects on vessel contents of the introduction of the batteries themselves and the chemicals they contain.

Circuitry inside such vessels could monitor one or more sensors monitoring vessel contents or conditions, and then transfer data gleaned back to the exterior of the container on a periodic basis. High data rates or continuous transmission are not typically necessary for these applications or compatible with these requirements. The combination of energy harvesting methods combined with low-power electronics is a an attractive combination for such applications.

In many situations the walls of the vessel or container of interest are made from steel, stainless steel, or some other metal alloy. This severely limits the applicability of traditional radio-frequency (RF) techniques because of the Faraday effects of sealed metal enclosures. The absence of direct mechanical access combine with the unsuitability of RF techniques points strongly to acoustic or ultrasonic methods, which is the subject of this report.

We demonstrate a custom ultrasonic modem that combines energy harvesting, power accumulation, and a simple data-modulation technique suitable for ultrasonic links through various solid metal barrier thicknesses. Extremely low standby power draw is also a feature of the demonstrated system. Using the demonstrated technique, interrogation of sensors inside a sealed vessel can be initiated remotely using only the application of the appropriate ultrasonics energy of the correct frequency to the external vessel wall to supply energy to the interior electronics. It is foreseen that long periods of latency can be tolerated by systems built on this principal, and that they would require very low maintenance.

The Ultrasonic Modem is designed as two subsystems as discussed and illustrated in the executive summary. One of these subsystems is an external module that transmits ultrasonic power through the vessel wall (herein also referred to a barrier), and which then listens for return signals upon the cessation of power transmission. The other is an internal subsystem or module that receives power through the vessel wall, stores the received energy, then triggers a sensing cycle and returns data from associated sensors using the ultrasonic link to the exterior environment. This report discusses the operation of these two subsystems in detail, providing test results and electronics details.

A brief literature review finds three papers showing demonstrations of or discussion pertaining to ultrasonic transmission through metal walls and barriers. Yang *et al* [1] give an account of efficient transfer of ultrasonic power through a 40-mm thick stainless steel plate, after which they were able to glean 15.7 watts of 5-VDC power from the interior electrical circuit. Their reported efficiency was 27.7%. Of note, this group used matching networks on both transmission and receiving systems in a similar way to our work, and also employ a novel resonant rectifier design. Yang *et al* do not return signals back through in the reverse direction, however. Primerano *et al* [2] discuss passing ultrasound through tank walls and bulkheads, and discuss the challenges of acoustic echoes in passing digital data across such barriers (intersymbol interference). Interestingly, they devised an echo cancellation technique which significantly improves their data transfer efficiency.

Of the three papers mentioned, Tseng *et al* [3] show a system most similar to ours in concept, although with a specific focus on embedding sensors completely within metal for industrial monitoring applications to detect *in situ* the onset of cracking and metal fatigue. Tseng *et al* obtain one-way power and two-way data transfer using a single PZ transducer for both power and data on each side of their transceiver in the same way we do, except currently our data channel only works in one direction (from interior to exterior, or the reverse direction to power transfer). They achieve 33% power transfer at 440 kHz over a 40-mm thickness of low temperature melting point fusible alloy that they use to cast around their two ultrasonic transducers. Tseng *et al* also present a fairly comprehensive literature review worthy of deeper study, including work that covers the in-depth modeling of communication between transducers in these situations.

By comparison, our system does not boast any such efficiency as the above-mentioned publications at this stage. However, to the best of our knowledge, our work is the first to demonstrate a working power and data channel through 36 inches of stainless steel.

1.1 Report Layout

This report proceeds from this introduction (Section 1) with a description of the interior subsystem in Section 2, the exterior subsystem in Section 3, and then system performance in Section 4. Next steps are then considered in Section 5, and conclusions are given in Section 6.

Please note that this report uses hyperlinks for items in the Contents, the short figure captions in the List of Figures, figure and section references throughout the text, as well as literature citations. Hyperlink text is shown as brown for ease of identification. Hovering over these links with the mouse while viewing the pdf file will show a preview of these items or sections, while clicking on them will navigate directly to them.

Acronyms included in the acronyms and definitions table are spelled out explicitly in the

text at first appearance, except where it was deemed distracting to do so. In the latter case, definitions are included as footnotes at first appearance.

1.2 Acknowledgement

This work is supported by the U.S. Department of Energy Packaging Certification Program, Office of Packaging and Transportation, Office of Environmental Management, under Contract No. DE-ACC05-76RL01830.

2 Interior Subsystem

The interior subsystem consists of two functional circuit-blocks: the harvester circuit and the processor circuit. These two circuit-blocks share a single piezoelectric (PZ) ultrasonic transducer that is effectively switched between the two circuits. The harvester circuit absorbs power coming in through the barrier and stores it on a large capacitor, and the processor gathers data from sensors, which is then transmitted back out through the barrier.

Figure 2.1: Example of the ultrasonic transducer type used for both the interior and exterior circuitry, Olympus V101.

The transducer used for both interior and exterior subsystems is an Olympus model V101, specified as a 500-kHz device, an example of which is shown in Figure 2.1. The interior transducer is connected to the Harvesting and Data Transmit circuitry shown in Figure 2.2 via BNC.* Solid state relays (U1 and U3) in this circuit switch the transducer between two pathways, allowing it to alternatively receive power from, and transmit data back to the external subsystem.

During the harvesting phase, the voltage waveform from the transducer is stepped up with a small transformer, T1 (EPCOS/TDK), and then rectified by a full-wave Schottky bridge formed by the two diode pairs D1 and D2. This signal is passed to a storage capacitor (via port +V_UT), shown as C6 in Figure 2.5, a 20-Farad lithium-ion supercapacitor (Taiyo Yuden LIC1030RS3R8206). This massive capacitance allows

*BNC: British naval connector

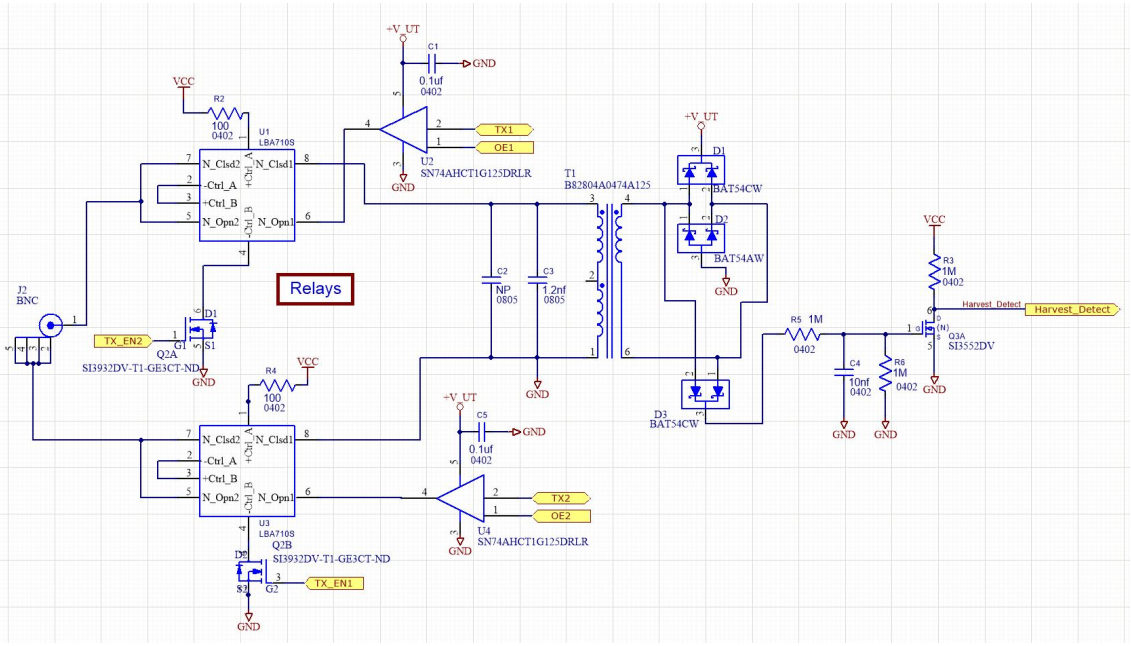

Figure 2.2: Harvesting and data transmit circuitry.

significant energy to be added to the system with minimal voltage variation, thus improving predictability and minimizing charge management requirements for the system.

A zero-power detection circuit (formed by diode pair D3, MOSFET Q3A and surrounding R's and C's in Figure 2.2) provides a signal indicating the termination of the harvesting cycle. This is the `Harvest_Detect` signal used to cue the microcontroller to switch the transducer cycle to data transmission mode.

Power Harvesting

The low leakage current of the supercapacitor combined with ultra-low sleep current of the microcontroller allows us to minimize the power transmit cycle time because the capacitor doesn't need to be recharged from 0 V every cycle. The capacitor's maximum voltage rating (3.5 V at 85C) allows us to maximize data transmit power without using step-up converters, and is well matched to the microcontroller specifications. The ease of gauging stored energy and extended temperature specifications make the supercapacitor preferable to a lithium ion battery.

Data Transmission

In transmit mode, the microcontroller passes data as a 9600-baud UART* signal, encoded using single-pulse-per-bit modulation, to the transducer via two SN74AHCT1G125 buffer/line drivers, U2 and U4. Every logic-low bit (including the

*Universal asynchronous receiver/transmitter

start bit) is represented as a single pulse at the beginning of the bit period. Logic lows are represented by pulses rather than logic highs because the UART idle state is logic high. (Please note that this is conflict with what was stated in the Executive Summary. This is because the inverted nature described here can be counterintuitive, and as such can complicate high-level explanations.) The exterior subsystem of the ultrasonic modem receives these pulses and amplifies them, and extends them to about 80% of a bit period using a monostable multivibrator. When inverted, the result is a valid UART signal due to UART oversampling. Not filling the entire bit period with pulses generated by the interior subsystem (as is done in the traditional ASK modulation) enables significant energy savings.

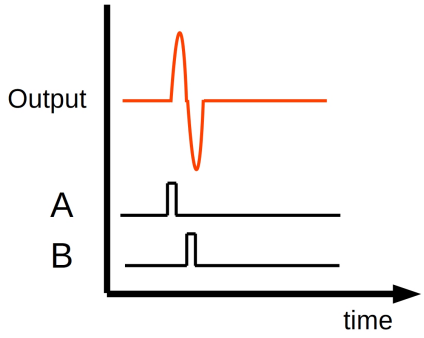

Figure 2.3: Transmit pulse-drive for transducer.

The pulse is generated using a bipolar drive method as illustrated in Figure 2.3, where both transducer terminals are controlled independently, and change state simultaneously in the opposite directions during the transition. This lets us double the apparent voltage that the transducer "sees" vs the available supply voltage. The transducer can also be driven in a unipolar fashion to conserve energy if that provides sufficient received signal amplitude.

Microcontroller

The microcontroller is the core of the interior subsystem. It sleeps most of the time, conserving power with a tiny current draw less than 50nA. The `Harvest_Detect` signal asserts when the exterior subsystem stops supplying power to start the data cycle. The microcontroller wakes ups, takes data from the sensors and formats a data message. The solid-state relays (U1 and U3 in Figure 2.2) are configured to connect the transfer (TX) buffer outputs (U2 and U4) to the transducer, and the data packet is then transmitted by driving pulses into the transducer as shown in Figure 2.3. After the data packet has been sent, the solid-state relays are reconfigured to connect the transducer to the power harvesting circuit, and the microcontroller goes back to a low-power deep sleep.

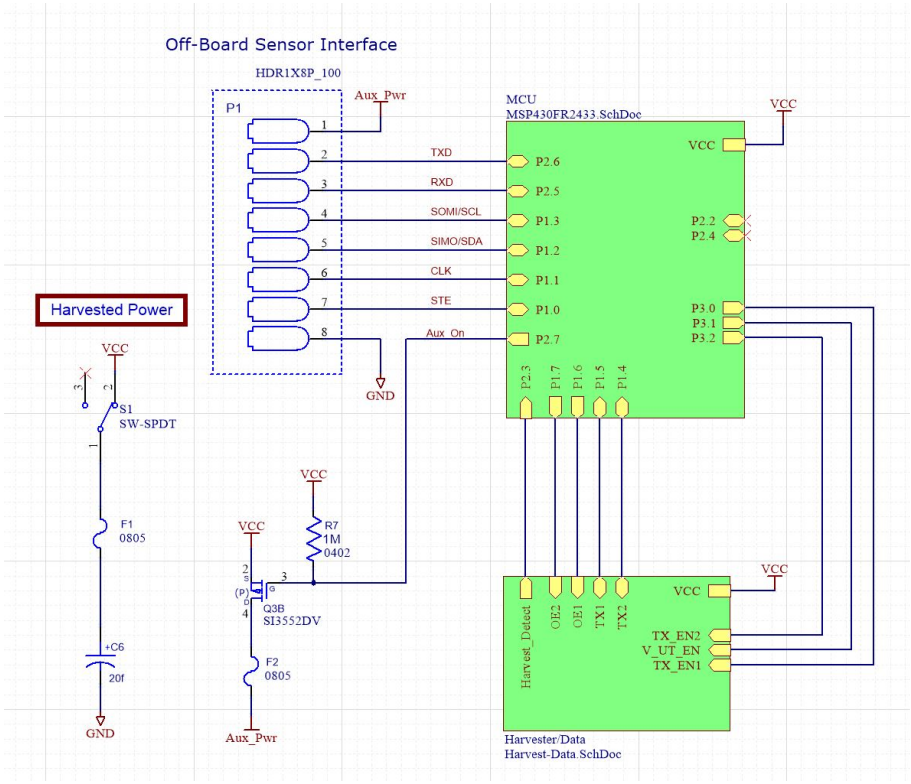

Figure 2.4: Main inside-modem circuit modules.

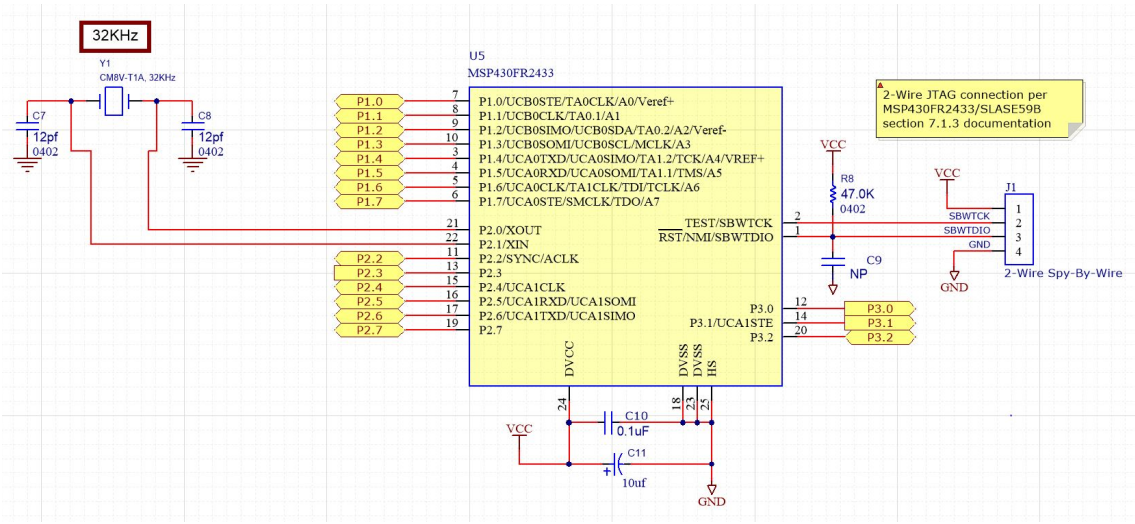

Figure 2.5: Microcontroller circuit.

3 Exterior Subsystem

The exterior subsystem consists of two parts, a power transmitter and a data receiver, as shown in Figure 3.1. As discussed previously, both these parts employ a common ultrasonic transducer, which, in the demonstrations to date is identical to that in the interior circuitry (Olympus model V101).

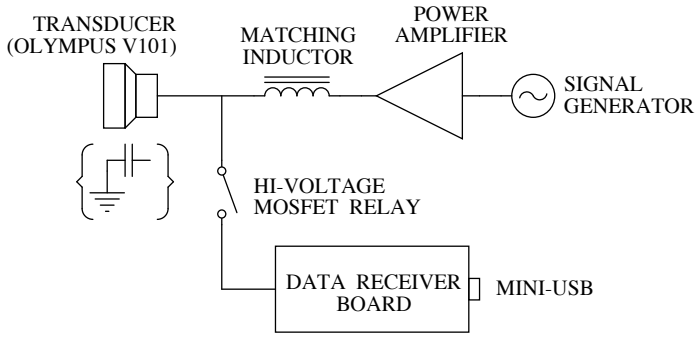

Figure 3.1: Overview of exterior subsystem.

The power transmitter is an RF drive chain presently consisting of a sine-wave signal generator, a custom power amplifier and an impedance-matching inductor. The ultrasonic transducer, although stated as being peaked for 500 kHz doesn't show strongly distinctive behavior at this frequency, as will be discussed in Section 3.1. Furthermore, the dominant characteristic of the transducer is capacitive, as indicated by the bracketed capacitor-to-ground symbol. The matching inductor forms a series resonance with this capacitance, greatly increasing the voltage appearing across the transducer for a narrow band of operating frequencies. The results of this action are a matched RF drive to the transducer, yielding very minimal reflected power (we couldn't detect any with the power meter we were using), meaning that acoustic power transmission efficiency through the steel barrier is maximized. The resulting load impedance as seen at the input to the matching inductor (or equivalently at the output of the power amplifier) is sufficiently close to 50 Ω to allow operation from a standard RF amplifier if so desired.

The operation of the system is currently envisaged as providing power transmission for a manually selected period of time, after which, the power transmit circuit is turned off. As discussed in Section 2, the interior subsystem detects the end of the harvesting cycle, and begins to transmit data back through the barrier via the interior transducer. This

continues while there is sufficient charge on the supercapacitor to do so (until its voltage falls to 3.3 volts). At the original inception of this project, the power transmission to data received ratio behavior was envisioned as something akin to that shown in Figure 3.2. However, we have seen the system supply data back for almost the same period of time (around five minutes) as it was given power.

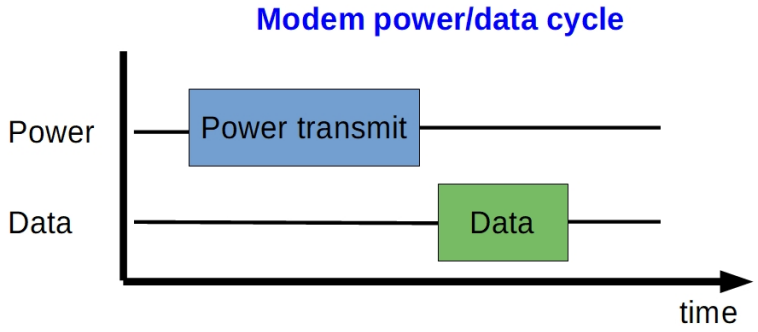

Figure 3.2: Power harvesting and data transmit cycle.

The transmit system is "turned off" by turning off the signal generator in the RF drive chain (see Figure 3.1), but leaving the power amplifier active.* This has the effect of actively holding the amplifier-end of the matching inductor at ground level, but allowing the node between the inductor and the transducer to move freely in the resonance band around 500 kHz. This means that it's not necessary to break RF power chain in order to receive data from the transducer. This is serendipitous because inserting a high-voltage switch into the middle of a resonant circuit sensitive to loss is problematic. All that is necessary in fact, is to activate a high-impedance probe circuit at that point, which in this case consists of an optically activated MOSFET relay, (IXYS LCA127), connecting this node to the high impedance input of the data receiver board. The data returning to the ultrasonic transducer is centered around 500 kHz, which resonates the LC-circuit† formed by the transducer and matching inductor, producing high fidelity signals despite the output of the amplifier being an active ground.

(The other option we tried was to use a 50-Ω high-voltage RF switch (Pasternack PE71S6405), to select more decisively between the drive chain and data receiver board. Because this unit was made to select between two 50-Ω sources, in order to protect these circuits it connects 50 Ω across the un-selected port. This didn't play well with the amplifier in the chain.)

The details of RF drive chain and characterization of the ultrasonic transducer are discussed in more detail in Section 3.1, while the circuitry in the data receiver board is

*This is somewhat different to what was presented in the executive summary, which was not focused on technical details.

†LC stands for an inductor-capacitor combination. An LC-circuit comprises inductors and capacitors.

discussed in more detail in Section 3.2.

3.1 Power Transmission Circuit

In this section we will discuss measurements pertaining to the impedance of the Olympus V101 ultrasonic transducer, details of the Matching Inductor and also the Power Amplifier shown in Figure 3.1. The only item not discussed herein is the Signal Generator, which was a Keysight function generator, model 33500B, but which could have been any of a large range of lab bench signal generators allowing operation at 500 kHz.

In order to understand how best to drive the ultrasonic transducer shown in Figure 2.1, its impedance was measured using an HP-4294A impedance analyzer. The magnitude and phase of this impedance is shown in Figure 3.3.

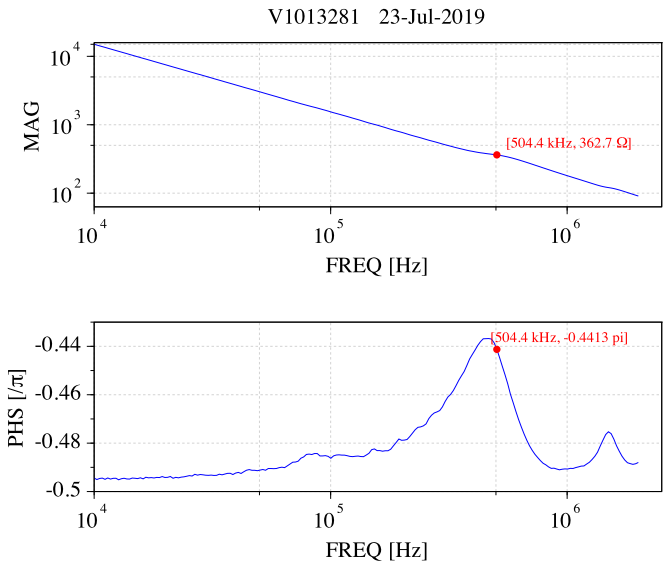

Figure 3.3: Impedance magnitude and phase of the Olympus V101 transducer.

This graph confirms that the impedance of the transducer is strongly capacitive, indicated by the falling impedance magnitude decade for decade in frequency, and also the general phase value in the vicinity of $-\pi/2$ radians, or $-90°$. While sold as a 500-kHz transducer, its electrical behavior near 500 kHz is not particularly striking. In other words there are no sharp amplitude features near 500 kHz, such as a strong peak or dip as might be seen with other transducers. There is a feature in the phase response, but the scale of the graph shows that it too is also relative weak, being only $\sim 0.06\pi$ radians in deviation. (Strong resonances in piezo transducers have phase responses that

move from $-\pi/2$ to $+\pi/2$ and back again through the resonance.) What this means is that electrically at least, this transducer looks broadband. We would therefore not have any problem driving it at frequencies somewhat different from 500 kHz. Indeed, our experience confirms that this transducer seems to operate well at frequencies out to 600 kHz, although we haven't tested the limits to its operating bandwidth.

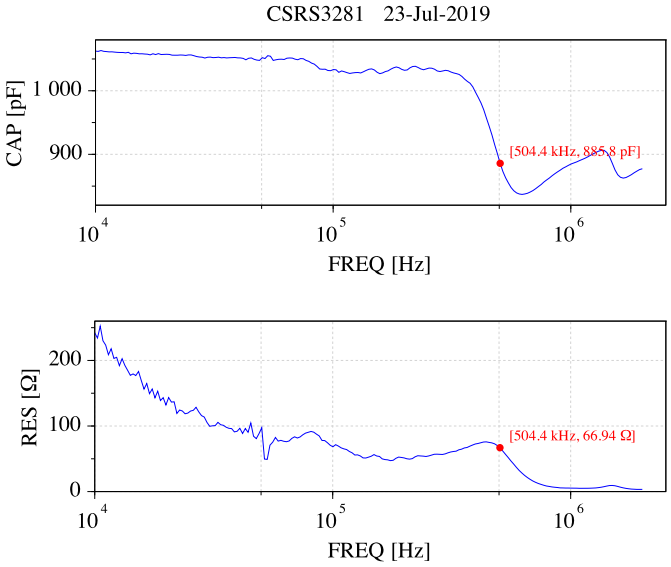

Figure 3.4: Impedance plot of Olympus V101 transducer showing projection onto hypothetical series capacitance and resistance.

What is more significant about the plot in Figure 3.3 is that the effective impedance at 500 kHz is 363 Ω. This means that it is an extremely poor match to any 50-Ω RF amplifier. Moreover, since this impedance is strongly capacitive, nearly all the power supplied by any such RF amplifier would be reflected back to the output stage, potentially jeopardizing the health of the amplifier. Earlier testing on this project without using a matching inductor were performed using a large power amplifier (ENI 2200L) designed to be robust to heavily mismatched loads, showed typical power transfer numbers of 24 watts forward and 22 watts reverse in order to produce 200 volts peak-to-peak (Vpp) across the transducer. This indicates that only 2 watts was being used by the transducer to generate acoustic energy, while the remaining 22 watts was being reflected back to be dissipated in the output stage of the power amplifier. In the case of the ENI 2200L, it is big enough* to not be adversely affected by this reflection. However, smaller amplifiers used with this application could well be destroyed by these reverse power levels.

This behavior strongly indicates the need for an inductive matching network. Projecting

*ENI 2200L: 200-W class-A RF amplifier, output protected, (H×W×D): 5.3"×16.5"×18.4" (134.5 mm ×420 mm×467 mm); 45 lbs (20.5 kg).

this impedance onto a hypothetical series capacitor-resistor pair gives us the plot shown in Figure 3.4. At 500 kHz, we see an apparent capacitance of 886 pF and a resistance of 67 Ω. If we can expose the latter real impedance to the output of the power amplifier, it's actually a reasonable match for a 50-Ω amplifier. Doing so is achieved by resonating the apparent capacitance with an inductor. For 500 kHz, in theory this inductor would be about 115 µH.

For various reasons,* and after trying various different designs, the inductor we ended up using was hand wound onto a T-157-15 powdered iron core, using 47 turns of AWG16 wire. Its inductance was measured as 81.58 µH, somewhat lower than the required estimate above. This inductor resonated the transducer at about 590 kHz, which was within the range over which we had tested the transducer. The hand-wound inductor is shown in Figure 3.5. Mounting it in a die-cast aluminum box reduced the magnetic coupling to other sources, while surrounding it with cardboard reduced the impact of the proximity of the metal box on the value of the inductor.

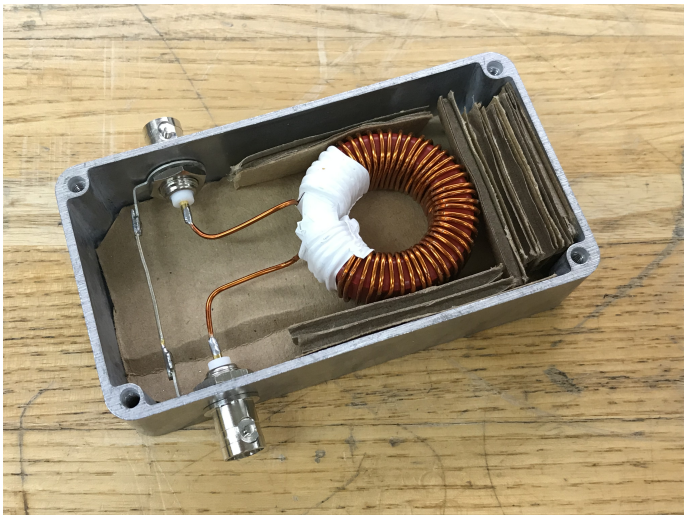

Figure 3.5: Hand-wound matching inductor for the Olympus V101 transducer. T-157-15 core, 47 turns of AWG16 wire, 81.58 µH.

Inserting the inductor into the transmit circuit between the amplifier and ultrasonic transducer as shown in Figure 3.1, allowed the same amplifier (ENI 2200L) to develop 200 Vpp across the transducer for only two watts forward, with no measured reverse power, indicating excellent matching between the 50-Ω amplifier and the ultrasonic transducer. Furthermore, this indicated that an amplifier of only a two-watt output power specification would be necessary to drive the transducer, paving the way for

*One such reason was to keep the ends of the inductor coil away from each other to avoid stray capacitance from affecting the resonance. A compounding factor was that we couldn't quickly find any healthy AWG20 (thinner) wire, which was first going to be used for a slightly higher inductance.

miniaturizing the final design of systems based on this technology.

This in turn allowed the large ENI 2200L power amplifier to be replaced with the one indicated below in Figure 3.6. This amplifier is a single integrated circuit design, using the Apex Microtechnology PA09U power amplifier chip* as a low impedance driver. The schematic for this circuit showing the amplifier plus the few required external components, is shown in Figure 3.7.

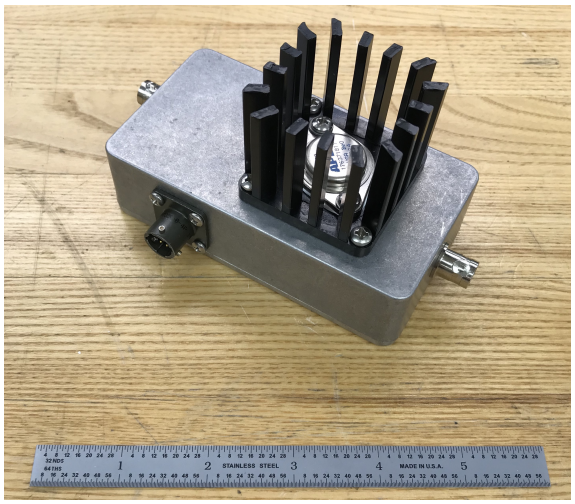

Figure 3.6: Photograph of custom amplifier mounted in aluminum die-cast box.

*https://www.apexanalog.com/products/pa09.html, datasheet https://www.apexanalog.com/resources/products/pa09u.pdf

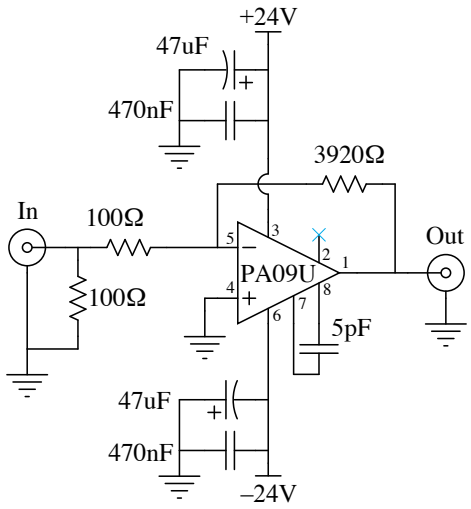

Figure 3.7: Schematic of custom amplifier for Olympus V101 transducer. Apex PA09U, configured for a voltage gain of 41.67, or 32.4 dB.

With the present configuration incorporating the PA09U, we found it produced 25 Vpp into 50 Ω for 600 mVpp at the input. This gives a voltage gain of 41.67, or 32.4 dB. The operating bandwidth under these conditions is approximately 1.6 MHz, more than adequate for our application at 500 kHz. The output swing of the PA09U requires seven to eight volts clearance from the power supply rails to avoid distortion. This is one aspect of these amplifiers that is different to other (lower power) operation amplifiers for example, which can go to within a volt or two of the power supply rails. Running from ±24 VDC, this means that our maximum output swing would be around 32 Vpp ($2 \times 24 - 2 \times 8 = 32$). This was confirmed by bringing the input voltage to 800 mVpp, getting 31 Vpp out, which was showing a couple of dB gain compression. At these levels we can only go to 700 kHz without distortion, however. At our required power of two watts we require 28.4 Vpp into 50 Ω, we achieve with sufficient margin.

(A higher bandwidth Apex amplifier, the PA119U, was also tested. It had similar performance to the PA09U, except it went out to 2.5 MHz under these conditions. The PA119U would be more suitable for higher frequency applications discussed in Section 5.)

3.2 Data Receiver

Figure 3.8 shows a block diagram of the data receiver electronics, including an amplifier block, envelope detector and miniUSB driver (with an intervening amplifier stage). These pieces are discussed in turn below.

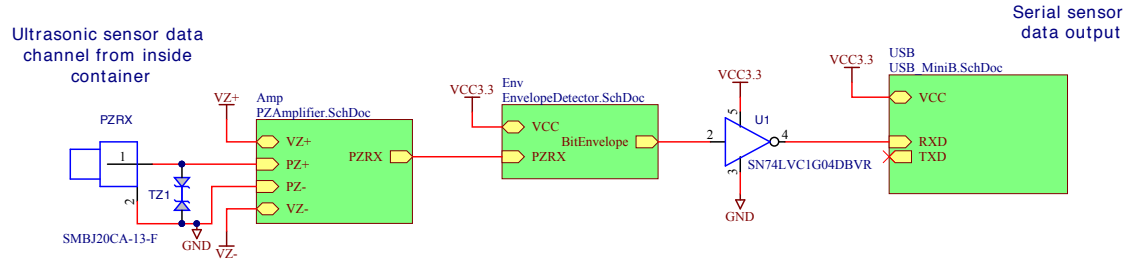

Figure 3.8: High-level block diagram of the data receiver.

The amplifier module shown in Figure 3.9 consists of two non-inverting stages allowing selection between two preset gains through the use of jumper pins. There is also provision for capacitive roll off if required, by added capacitors across the gain networks. A table of total expected gains for various jumper positions is also included. This was the initial configuration of these amplifier stages and is included here more as an example of how this could be done, rather than a definitive description. As we changed the barrier thickness, the gain settings frequently had to be changed, and ultimately further than allowed by this configuration. As a result we ended up replacing R1 and R2 with 4.99 kΩ , and using 100 kΩ potentiometers for RA1 and RB1. We didn't put this in this schematic for two reasons: firstly, it wasn't the configuration used for most of our work (the one shown was). Secondly, this configuration is not final either. Ultimately, in any operational system, some kind of automatic gain control mechanism would be necessary for this front stage. This is addressed in Next Steps, Section 5.

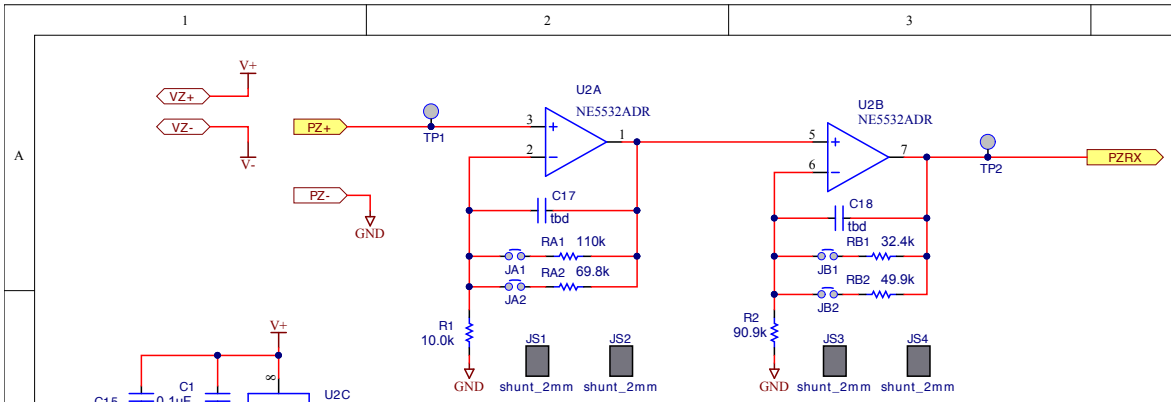

Piezo Amplifier Selectable Gain

Jumper Selectable Section Gain		
$G_{A1} = 12$	$G_{A2} = 8$	$G_{A3} = 4$ (RA1 || RA2)
$G_{B1} = 10$	$G_{B2} = 6$	$G_{B3} = 4$ (RB1 || RB2)

Combination	Overall Amplification	JA1	JA2	JB1	JB2
$G_{A3}G_{B3}$	4 X 4 = 16		X	X	X
$G_{A3}G_{B2}$	4 X 6 = 24		X		X
$G_{A2}G_{B3}$	8 X 4 = 32		X	X	X
$G_{A3}G_{B1}$	4 X 10 = 40		X	X	
$G_{A2}G_{B2}$	8 X 6 = 48		X		X
$G_{A1}G_{B3}$	12 X 4 = 48	X		X	X
$G_{A1}G_{B2}$	12 X 6 = 72	X			X
$G_{A2}G_{B1}$	8 X 10 = 80		X	X	
$G_{A1}G_{B1}$	12 X 10 = 100	X		X	

Title: PZAmplifier.SchDoc			Battelle/PNNL PO Box 999 MS K5-17 Richland, WA 99352 USA
Size: A	Number: 2	Revision: 1.0.0	
Date:	Time:	Sheet 2 of 5	
File: C:\Users\dunn874\AppData\Local\Temp\Snapshot\2\PZAmplifier.SchDoc			
Engineer: R Dunn		Created: 22 Aug 2018	
Drawn By:		Updated: 30 Aug 2018	
Checked By:		Released: 31 Aug 2018	

Figure 3.9: This figure shows the configurable amplifier block for the Exterior Subsystem Receiver.

The envelope detector is the key circuit that turns the variable sized ultrasonic pulses into a standard RS232 format. An ultrasonic pulse received by the transducer is turned into an equivalent voltage pulse, which is first amplified and rectified before being applied to the envelope detector. Amplification of the pulse is necessary to bring the voltage up to a range usable by the digital detector circuit. Rectification is also necessary since the digital circuitry doesn't respond to negative voltages. This amplified and rectified signal is shown as the Detector input signal in 3.11 in red. This pulse by itself isn't long enough to be interpreted as a valid RS232 bit. The envelope detector chip is triggered by the leading edge of the pulse to change state, and then maintains the triggered state for a time period that can be interpreted as a valid RS232 bit, shown as the Bit envelope in 3.11 in black.

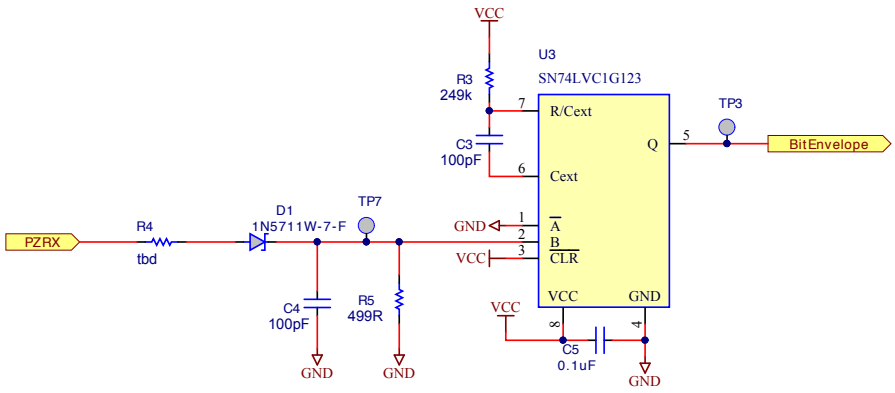

Figure 3.10: Data receiver envelope detector circuit.

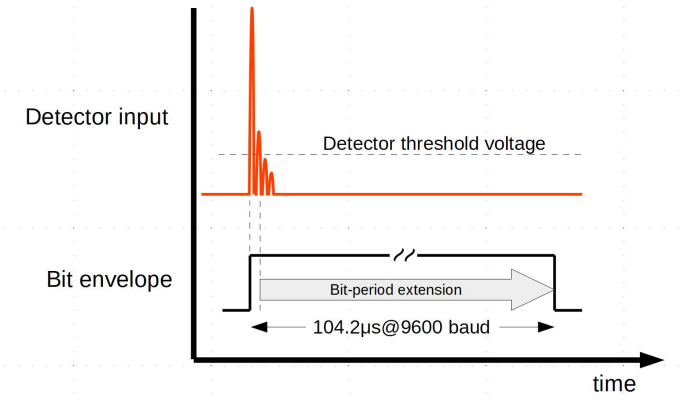

Figure 3.11: This figure shows the action of the bit envelope detector, which is to extend received pulses to fill most (80%) of the bit-period.

To be compatible with almost any computer system, the output of the modem receiver is in the form of an RS232 data stream in what's known as 9600,n,8,1 format.* This is a very common data communications stream that can be used as is, or easily turned into another form by common interface chips. For simplicity of testing with modern laptop computers, the RS232 data stream is converted to USB format using an FTDI FT230XS-R chip. The output of the Envelope detector circuit is inverted to comply with the expected TTL-level RS232 signal, and then fed into the FTDI chip that converts the data into USB format that can be plugged directly into a laptop computer.

*9600,n,8,1 format, or 9600/8-N-1, is a common shorthand notation for serial port parameter settings in asynchronous mode, meaning that there is one start bit, eight (8) data bits, no (N) parity bit, and one (1) stop bit.

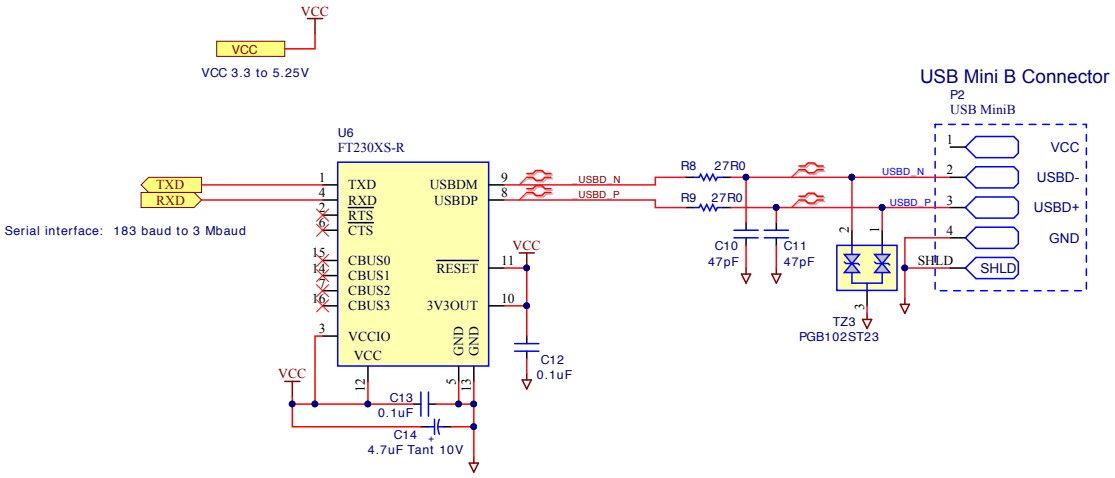

Figure 3.12: Data receiver serial port / USB modem interface.

4 Performance

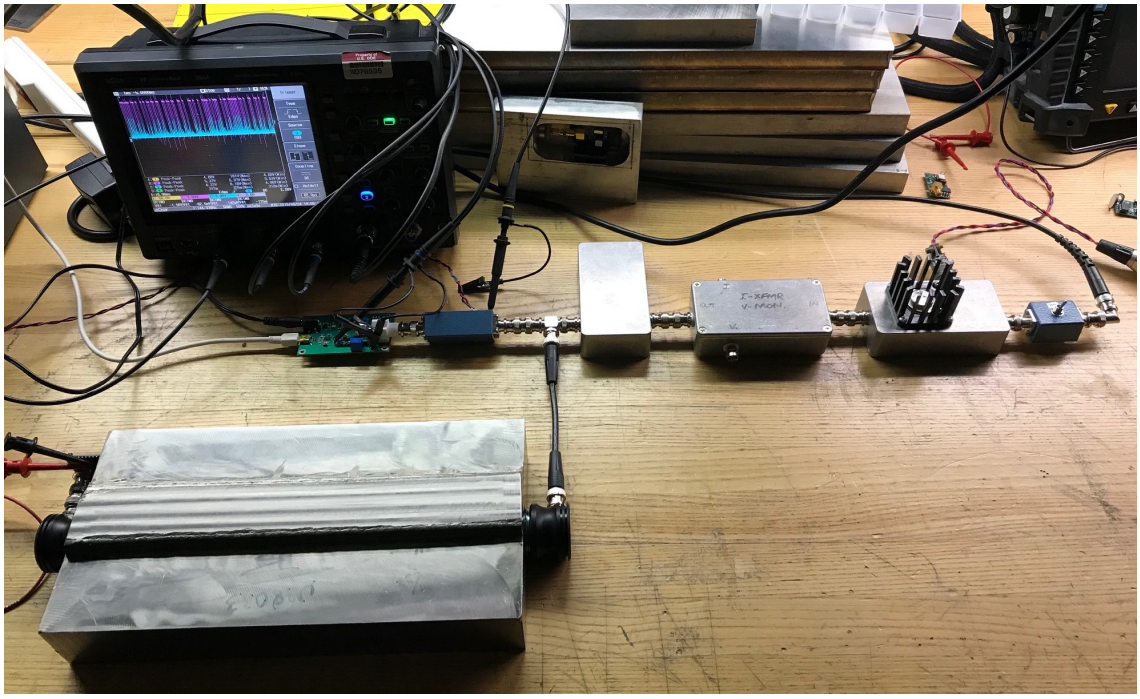

Figure 4.1: Experimental setup with a 12-inch steel barrier.

Figure 4.1 shows the full experimental setup with a one-foot piece of stainless steel as the intervening barrier between the two ultrasonic transducer elements. Moving from the right to left focusing on the chain of metal boxes, the small blue box to the right is an on-off switch box used to protect the amplifiers in the chain. This switch box feeds a sine wave signal from the signal generator (off screen, connected via BNC cable) to the custom amplifier module (box with the vertical heatsink fins). The output of this amplifier is passed through two more metal boxes to the ultrasonic transducer. The first of these (horizontal box) is a voltage and current monitor circuit, not discussed further in this report. The second is the matching inductor. As mentioned previously, the data received back through the steel block is taken from the node between the ultrasonic transducer and the matching inductor. This is seen in this photograph as the BNC T-piece connecting the ultrasonic transducer not only to the inductor, but also to the second small blue box to the left. This second blue box contains the Hi-Voltage MOSFET Relay mentioned previously and shown in Figure 3.1. (Presently this relay is

operated by manually supplying it with a control voltage from a separate power supply. In a full system this will be operated by the microcontroller.) The data Receiver Board (green printed circuit board (PCB) immediately in front of the oscilloscope) to the left of this unit receives the electrical signals from the ultrasonic transducer when this relay is activated. Probe leads allow the oscilloscope to record raw and processed digital signals from the Data Receiver Board during periods when the system is in data-receive mode, yielding the cyan and magenta traces on the scope.

The interior electronics described in Section 2 is mounted on a small PCB connected to the ultrasonic transducer shown on the left-hand side of the block.

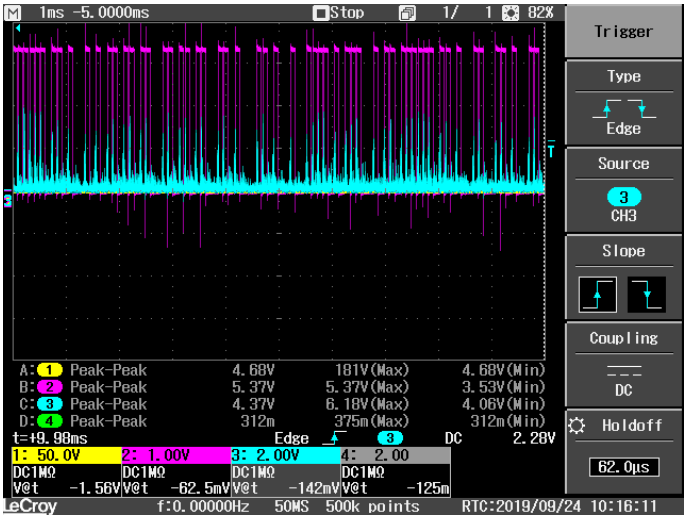

Figure 4.2: Screenshot of data transfer. Timebase: 1 ms.

Figure 4.2 shows a screen shot of the oscilloscope screen taken when the exterior circuitry is receiving data through the 12-inch block. The cyan trace is the amplified and rectified transducer output; the magenta trace is the output of the one-shot pulse extender (peak detector). These two signals were taken from test points TP7 and TP3 respectively of the Data Receiver Board shown in Figure 3.10. The effect of pulse extender in taking the raw received signal and yielding a more recognizable digital signal is clear. A single bit is a single pulse shown on the magenta trace. The pulse width is set to be approximately 80% of the maximum possible bit width at a data rate of 9600 baud. The entire shot captures a little under eight bytes of data.

(Sometimes an echo or noise re-trigger the one-shot pulse extender. This is why the pulse widths in its output are not uniform, and why the separation between the pulses is inconsistent. UART oversampling prevents this from being a problem. Whatever state the signal is in more than 50% of the time is what the UART reads it to be.)

Figure 4.3: Experimental setup with a 36-inch steel barrier.

Figure 4.3 shows the same experimental setup, but for a 36-inch stainless steel barrier between the two transducers. (There were three similarly sized 36-inch blocks of stainless steel on the same pallet. We're only using the one towards the top of the figure as a test block, while the other two serve to support our equipment.) The same power transmit and data receive (external) circuitry is seen to the right-hand side of the metal blocks, while the self-contained internal circuitry is seen to the left-hand side. Returned data is seen on the oscilloscope screen.

Figure 4.4 shows the data received by the Tera Term application on the PC plugged into the miniUSB port of the Data Receiver Board, for both the 12-inch block (4.4a) and the 36-inch block (4.4b). The microcontroller was programmed to return the temperature in degrees Celsius and the voltage on the supercapacitor, these two screen shots clearly showing success in both cases. There is some obvious data fidelity loss in the case of the 36-inch block, which is not surprising, and can be removed with fine tuning. Even as it is the data is discernible and usable. The gain settings on the Data Receiver Board had to be frequently adjusted, ultimately prompting us to replace certain resistors on the board with potentiometers as discussed in Section 3.2.

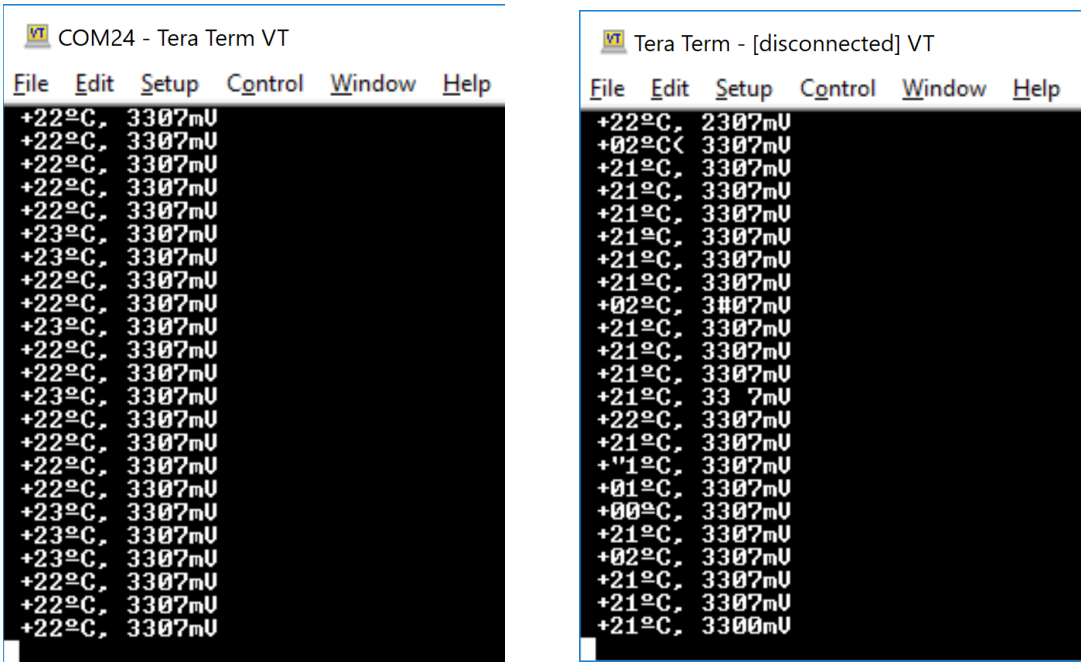

(a) (b)

Figure 4.4: Tera Term output for data transmitted through the 12-inch (a) and 36-inch (b) stainless steel test blocks. The columns show ambient temperature and the voltage across the super capacitor. There is some minor loss of fidelity in the 36-inch case but the transmission is still very clear.

Power transfer and efficiency

Looking at power transfer numbers, for two watts of power supplied by the power transmit electronics, the power received by the internal electronics was measured to be 4.2 mW for the 12-inch block and 1.54 mW for the 36-inch block. This was done without any optimization of the voltage to current ratio, such as peak power tracking proposed in the Section 5. Preliminary testing of this technique has shown a potential three-fold improvement.

While not high efficiency numbers (0.21% and 0.077% respectively), these are (as far as we know) the best that's ever been demonstrated for this size of barrier. The energy accumulated through the 36-inch block in five minutes allows us to send data for 4.5 minutes before the supercapacitor discharges below 3.3 volts, which was the starting voltage of the harvesting cycle.

5 Next Steps

There are multiple directions we can go from this point in this project. We break this section down into three subsections: Short term, Medium term and Long term.

5.1 Short Term

Understanding Modal Structure
While optimizing operating frequencies when transmitting power through the 12-inch stainless steel block it was noticed that there were intense peaks and nulls in the response of the ultrasonic transducer receiving the transmitted power as the operating frequency was adjusted. For example, in one instance we saw a strong peak at 369.14 kHz, a slightly weaker one at 371.13 kHz, with several minor ones in between. The difference between these two major frequencies was 1.99 kHz. This doesn't correspond to any known spacing we understand regarding constructive interference within the geometry of the block. Our calculations show that the frequency separation of adjacent constructively enhanced length modes of the block should be about 9.5 kHz — quite different to what we have observed. (Our calculations used the speed of sound in steel of 5800 m/s.*)

Minor fluctuations in the transmission of power through the steel block are to be expected, and are not concerning in general if they are small to moderate in size. However, we are seeing moderate to large variations that could be problematic. In fact, we have identified particular operating frequencies yielding complete nulls in power transmission! (One example we saw for our 12-inch block was at 379.753 kHz.) This is disturbing, in that if we were to pick such a null by accident, it would completely impede the operation of any system, and could have give us entirely the wrong impression of the technique. In an application setting, picking such a frequency could result in a total misconception regarding the state of the internal electronics.

Perhaps more importantly than fully understanding the provenance of this structure, is understanding how it varies with different sizes and geometries of barrier. We could then understand how we would need to vary the operating frequency of the modem, and over what frequency range, in order to have the best chance of finding a good operating frequency for particular barrier characteristics. These observations have also led to the need for a frequency optimization sweep as part of the operation of any instrument based on this principal, covered more in Section 5.2.

*m/s = meters per second.

This exploration will involve testing barriers made from the same length of the same grade of stainless steel, but of different shapes or aspect ratio. This would indicate if the observed effects have to do with high-order geometric acoustic transmission modes through the block, or some other presently unaccounted for geometrical effect.

Deeper Literature Review and Modeling
As mentioned in the introduction (Section 1) the paper by Tseng *et al* [3] contains a significant literature review, which is worthy of deeper study. Tied to understanding modal structure of the steel barriers mentioned immediately above, is an assessment of the impact of some modeling. There are several existing directions of modeling in the literature, mentioned by Tseng *et al*, which could be explored with minimal effort.

Different or Irregular Barriers
So far we have only tested the behavior of this system with fairly uniform-grain stainless steel. It makes sense to do some tests on different materials, such as softer steels, and materials with welds in them. These tests would be easy to do, and depend simply on the availability of test pieces.

5.2 Medium Term

Much of the work to date has been performed with a very modular set of tools, which has been expedient for our proof of concept. One of the next steps is to fabricate dedicated boards for the Interior and Exterior circuits. This will go hand in hand with enhanced capabilities of both subsystems.

External Board
The most modular part of our experimental system to date has been the external circuitry, comprising the power transmit and data receiver circuitry. This has been because this part of the system embodied the biggest uncertainty. After establishing the operation of the amplifier and matching inductor, the pathway is now clear to make a dedicated external circuit board.

The external board will include the chosen amplifier, the matching inductor (shielded), the high-voltage relay and the data receiver circuitry, and any circuitry required to monitor the voltage and current delivered to the ultrasonic transducer.* The external board will include a microcontroller discussed in more detail below.

In all likelihood the custom amplifier would remain an Apex Microtechnologies PA09U high-current high-bandwidth power amplifier. There were thoughts originally to push the operating frequency of this system in general out to 3 MHz, which might require a different amplifier such as the PA119U, but this idea has since moved to the realm of long-term goals.

*Monitoring would be both before the matching inductor and at the ultrasonic transducer itself.

The board will likely require the same ±24 V rails currently used by the amplifier, which could be readily derived from the 48 VDC provided through standard Ethernet systems. This would facilitate the end goal of having a system powered simply by the same Ethernet connection ultimately used to pass data back to a remote system used to record data obtained from the ultrasonic modem.

External Subsystem Microcontroller

The proposed external board will include a microcontroller (proposed MSP430FR2355) to facilitate generating the signals required for the power transmission drive chain, to perform the first level of processing on the data received back through the barrier, and to communicate with the outside world. This microcontroller will also facilitate other features discussed below, including bidirectional communications between the external and internal subsystems, as well as power transmission frequency and amplitude optimization.

Work specifically related to the microcontroller will include rearranging the surrounding circuitry to make use of the onboard analog modules, accommodating any power supply requirements and signal level shifts, as well as writing the necessary firmware and software for this microcontroller.

Signal Generation

As mentioned previously, a Keysight signal generator is presently used to provide the signal to power transmission drive chain. As such, it has to be manually adjusted both in amplitude and frequency for a particular setup, arrangement or test barrier. This was acceptable for the proof of principal, but moving forward, this input signal needs to be generated by the above-mentioned microcontroller for several reasons, including performing frequency sweeps to identify the optimum end-to-end* transmission frequency for a given barrier, and then amplitude adjustment to maximize power transfer.†

Another reason signal generation needs to be passed to the proposed external microcontroller is that of the proposed bidirectional communication between the internal and external subsystems. This will in all likelihood be facilitated using amplitude shift keying (ASK), which involves amplitude-modulating the power transmission drive signal to encode the digital signal onto the power transmission.

Internal Subsystem Board

The internal circuitry is more complete than the external circuitry at this point, but it still requires revamping in the medium term. The proposed microcontroller for the internal circuitry would also be the MSP430FR2355, whose peripheral selection makes it well suited for the tasks required to run the system such as managing system power, handling communications to the exterior modem and off-board sensors, and coordinating

*End-to-end here means from the power transmission through to receiving this power within the interior circuitry, as opposed to an optimum based on the state of the transmission electronics alone.

†Amplitude optimization would likely be based solely on the voltage developed across the exterior ultrasonic transducer.

subsystem operation. New features and roles for the internal circuitry would include facilitating optimal harvest frequency selection. This might proceed by the internal circuitry recording levels of power received over some time period during harvesting, this time period initiated by the external circuitry (via ASK on the transmitted power) and then returning information at a later time about the maximum power transfer point, in turn allowing the external system to identify the corresponding frequency.

The proposed internal circuitry would facilitate peak power tracking, in which an auxiliary storage capacitor would be charged by the harvesting circuit, and allowed to rise in voltage to the point where the power derived from the harvesting circuit reaches a maximum. This usually happens at something like 12 volts or so. From there, a buck (voltage reduction) switch-mode regulator would couple this capacitor to the existing 3.5-volt supercapacitor in a controlled way, as to ensure the maximum power point is maintained. As mentioned previously, this promises to yield an increase in power transmission performance by a factor of three or four.

Another area of exploration for the internal circuitry is that of higher temperature operation. Currently, the supercapacitor is rated at 85°C , which is not particularly high. There are other capacitors with higher temperature ratings. These shall be explored. The proposed microcontroller above has a maximum operating temperature of 105°C. This would be a starting baseline for the entire internal circuit.

Different Frequencies; Different Transducers

In the testing described in this report we have used the Olympus V101 transducer exclusively, and have operated at frequencies near 500 kHz. There are other transducers available that would be worth testing in the near term to see if there are any major differences. It may also be worthwhile to test at lower operating frequencies that 500 kHz, down as low as 50 kHz if transducers are available, because losses in steel (and other materials) are proportional to frequency raised to some power, meaning that lower frequencies may yield better performance. Transducers tend to get larger and more expensive as frequencies drop, so there would be a natural limit to a system intended for portable or hand-held use.

Higher frequencies would yield less efficient sonic conduction but may afford a much smaller system footprint, both in terms of the transducer and electronic items such as the amplifier and inductor. However, the high frequency exploration has been moved to the long term goals section.

Exploration of advanced techniques may also be a medium-term goal, including such things as the echo cancellation scheme of Primerano *et al.* [2] This would go hand in hand with, and would depend on, decisions made with regards to modeling mentioned above in the short-term goals.

5.3 Long Term

The long-term goals of this project include operation of the internal circuitry at much higher temperatures, perhaps up to several hundred °C. This is very difficult for microcontrollers, and may in fact have to be an entirely passive circuit, such as an ultrasonic transducer and a simple LC resonance. This is definitely beyond the short and medium term scope described above, and will be discussed at a later date.

Apart from higher temperature, another direction to pursue is a miniature, compact hand-held system. This would necessitate going to higher frequencies to reduce transducer size despite the inherent loss of efficiency through solids such as stainless steel. This could be explored towards the end of this work in a progressive manner, beginning with exploring identified transducers that operated up to 3 MHz.

6 Conclusion

In this report we have shown the successful demonstration of the transmission of both power and data through both 12- and 36-inch long blocks of stainless steel, paving the way for remote interrogation of the contents of vessels or the status of otherwise inaccessible industrial machinery or processes, through thick walls or barriers. The system demonstrated, the dual-path ultrasonic modem, has two subsystems: an exterior and an interior subsystem. The exterior subsystem provides ultrasonic power when required by the user, which is then harvested by the interior subsystem. The resulting stored energy is then used to interrogate sensors, and send data back through the barrier where it is received by the external subsystem and displayed or recorded. The system we have demonstrated also shows the potential to remain viable for long periods of time without interrogation, making the idea suitable to health monitoring systems of isolated systems in deep storage, for example.

There are multiple directions to pursue subsequent to this work, including enhancements to the system's efficiency, robustness and versatility. There are also areas of research to pursue to answer questions and issues uncovered during this work, such as the modal structure observed of the stainless steel blocks used, which caused signal nulls at certain frequencies. An important future area of study would involving operating the interior subsystem at elevated temperatures (and pressures), leading to the potential application of this technology to hostile environments. The possibility of a hand-held external interrogator subsystem could also be pursued.

7 References

[1] H. Yang, M. Wu, Z. Yu, and J. Yang, "An Ultrasonic Through-Metal-Wall Power Transfer System with Retgulated DC Output," *Applied Sciences*, vol. 8, no. 692, April 2018.

[2] R. Primerano, M. Kam, and K. Dandekar, "High Bit Rate Ultrasonic Communications through Metal Channels," in *2009 43rd Annual Conference on Information Sciences and Systems*, Drexel University. IEEE, March 2009, pp. 902–906.

[3] V. F.-G. Tseng, S. S. Behair, and N. Lazarus, "Acoustic Power Transfer and Communication With a Wireless Sensor Embedded Within Metal," *IEEE Sensors*, vol. 18, no. 13, pp. 5550–5558, July 2018.

Pacific Northwest
NATIONAL LABORATORY

U.S. DEPARTMENT OF
ENERGY

902 Battelle Boulevard
P.O. Box 999
Richland, WA 99352
1-888-375-PNNL (7665)
www.pnl.gov